ADVANCES IN ATMOSPHERIC SCIENCES, VOL. 32, MAY 2015, 613–623

Influence of Future Tropical Cyclone Track Changes on Their Basin-Wide Intensity over the Western North Pacific: Downscaled CMIP5 Projections

WANG Chao and WU Liguang*

Earth System Modeling Center and Pacific Typhoon Research Center, Key Laboratory of Meteorological Disaster of the Ministry of Education, Nanjing University of Information Science and Technology, Nanjing 210044

(Received 24 May 2014; revised 19 August 2014; accepted 5 September 2014)

ABSTRACT

The possible changes of tropical cyclone (TC) tracks and their influence on the future basin-wide intensity of TCs over the western North Pacific (WNP) are examined based on the projected large-scale environments derived from a selection of CMIP5 (Coupled Model Intercomparison Project Phase 5) models. Specific attention is paid to the performance of the CMIP5 climate models in simulating the large-scale environment for TC development over the WNP. A downscaling system including individual models for simulating the TC track and intensity is used to select the CMIP5 models and to simulate the TC activity in the future.

The assessment of the future track and intensity changes of TCs is based on the projected large-scale environment in the 21st century from a selection of nine CMIP5 climate models under the Representative Concentration Pathway 4.5 (RCP4.5) scenario. Due to changes in mean steering flows, the influence of TCs over the South China Sea area is projected to decrease, with an increasing number of TCs taking a northwestward track. Changes in prevailing tracks and their contribution to basin-wide intensity change show considerable inter-model variability. The influences of changes in prevailing track make a marked contribution to TC intensity change in some models, tending to counteract the effect of SST warming. This study suggests that attention should be paid to the simulated large-scale environment when assessing the future changes in regional TC activity based on climate models. In addition, the change in prevailing tracks should be considered when assessing future TC intensity change.

Key words: tropical cyclone track and intensity, climate change, downscaling, CMIP5

Citation: Wang, C., and L. G. Wu, 2015: Influence of future tropical cyclone track changes on their basin-wide intensity over the western North Pacific: Downscaled CMIP5 projections. *Adv. Atmos. Sci.*, **32**(5), 613–623, doi: 10.1007/s00376-014-4105-4.

1. Introduction

Tropical cyclones (TCs) account for the majority of loss of life and property induced by natural disasters, especially in the western North Pacific (WNP), which is the most active basin of TCs on Earth (Zhang et al., 2009). Thus, it is very important to know how TC activity responds to global climate change. Emanuel (1987) suggested that the maximum intensity of TCs would increase under a warmer climate. On the other hand, Wu and Wang (2008) found that the changes in TC genesis location and prevailing tracks are closely associated with increases in the percentage of intense TCs, suggesting that shifts in TC prevailing tracks play an important role in changes of basin-wide TC intensity. Kossin and Camargo (2009) demonstrated the importance of TC track change in recent increases in Atlantic TC activity, and suggested that track changes may offset the effect of increasing maximum potential intensity (MPI). Wing et al. (2007) found that changes in tracks play an importance role in intensity changes on the interannual time scale. Studies have shown that climate change will likely alter the TC tracks over the WNP (e.g., Wu and Wang, 2004; Wu et al., 2005; Li et al., 2010; Murakami et al., 2011). Considering the influence of changes in TC tracks on basin-wide intensity (Wing et al., 2007; Wu and Wang, 2008; Kossin and Camargo, 2009), it is necessary to assess its contribution to TC intensity.

Despite significant improvements in climate models, considerable biases in the simulated large-scale environment exist in current climate models (IPCC, 2007; Reichler and Kim, 2008; Knutson et al., 2013). It is clear that the reliability of the large-scale environment for TC activity simulated by each global climate model should be evaluated when the future changes of TC activity are assessed. Thus far, few studies have paid attention to evaluating the capability of CMIP5 (Coupled Model Intercomparison Project Phase 5) models in terms of the simulated large-scale environment important to

* Corresponding author: WU Liguang
Email: liguang@nuist.edu.cn

TC activity (Knutson et al., 2007, 2008; Emanuel et al., 2008; Bender et al., 2010; Emanuel, 2013). Given the dominant role of the large-scale environment on TC activity (Gray, 1968), it is clear that the selection of climate models is very important when downscaling TC activity with the climate model output. Recently, Knutson et al. (2013) demonstrated a large spread exists among individual models in their future projection experiment results. In a previous paper, Wang and Wu (2012) explored this issue using a theoretical dynamic downscaling system and suggested that large differences exist in the simulated large-scale conditions important for TC development.

In the above context, the primary objective of this study is to address the role of future TC track changes in TC intensity change using the model outputs from CMIP5 (Taylor et al., 2012).

2. Data and methods

2.1. *Data*

Wu and Zhao (2012) indicated that the intensity records in the Joint Typhoon Warning Center (JTWC) best-track dataset are more reliable than those from the Shanghai Typhoon Institute (STI) of the China Meteorological Administration, and the Regional Specialized Meteorological Center (RSMC) of Tokyo. For this reason, The JTWC best-track dataset for the period 1975–2005 is used to represent the observed TC activity. In this study, TCs refer to those in the JTWC dataset with at least tropical storm intensity (maximum wind speed exceeding 17.2 m s^{-1}), and our analysis is focused on the typhoon peak season (July–September). Monthly sea surface temperature (SST) from the National Oceanic and Atmospheric Administration (NOAA) (ERSSTV3b; Smith et al., 2008) is used in this study. Monthly atmospheric data are from the National Centers for Environmental Prediction–National Center for Atmospheric Research (NCEP–NCAR) reanalysis (Kalnay et al., 1996) dataset.

The output of the global climate simulations is from the CMIP5 multi-model dataset. In this study, the monthly data of two experiments [the historical experiment and Representative Concentration Pathway 4.5 (RCP4.5) experiment] are used for each model. The historical experiment is forced by observed conditions, which include changes in atmospheric composition, solar forcing, natural or anthropogenic aerosols, and so on. The radiative forcing in RCP4.5 experiment stabilizes at 4.5 W m^{-2} in 2100 (Taylor et al., 2012). To evaluate the performance of GCMs in their historical experiments against the reanalysis, all of the datasets are interpolated into $2.5^\circ \times 2.5^\circ$ grids.

2.2. *Downscaling technique*

A downscaling technique has developed over the past 15 years or so that involves embedding a high-resolution regional model in the atmosphere–ocean conditions derived from low-resolution global climate model output to study future intensity change (e.g., Knutson et al., 1998; Knutson and Tuleya, 2004; Knutson et al., 2007, 2008; Bender et al., 2010; Knutson et al., 2013). Currently, two specific approaches are used within this downscaling technique. One is to run a high-resolution regional model or hurricane model driven by large-scale conditions from climate models, and the TC climatology is determined by the activity of TC-like vortices simulated in the regional climate or hurricane model (Knutson et al., 2007, 2008; Bender et al., 2010, Knutson et al., 2013). The other is the theoretical dynamic system proposed by Emanuel et al. (2008). This system simulates TC activity by integrating the genesis, track and intensity models, forced by the large-scale conditions from reanalysis data or outputs from climate model simulations. Emanuel et al. (2008) applied this approach to simulate the global TC activities in the period 1980–2005 and assess the impact of climate change on TC climatology. The approach provides us with an efficient tool for assessing the impact of climate change on TC activity, enabling evaluations of the reliability of climate models in terms of the large-scale conditions for TC activity, and examinations of the contributions of each change in the large-scale conditions (Wang and Wu, 2012). Thus, the second approach is adopted in this study to investigate the roles of TC track changes in future TC intensity.

A similar downscaling approach to that described by Emanuel (2006) and Emanuel et al. (2008) is used in this study, and the TC characteristics are determined by the outputs of genesis, track and intensity models. Nevertheless, we use the TC genesis distribution derived from the JTWC best-track dataset in this study owing to the poor understanding of how such a distribution would change in a warmer climate (Emanuel, 2006; Knutson et al., 2010), especially in individual basins. The track model in the downscaling approach is adopted from Wu and Wang (2004). In this model, a TC is treated as a rigid body, and moves with the translation vector determined by the sum of mean beta drift and large-scale steering flow (pressure-weighted average wind from 850 to 300 hPa). Furthermore, random synoptic-scale disturbances are put into the translation vectors to take into account the possible effect of synoptic-scale weather systems on TC motion. The integration of the track model stops while the simulated TC location is out of the simulation domain (0°–40°N, 100°–180°E). The TC intensity model is an axisymmetric atmospheric model adopted from Emanuel et al. (2008). In this downscaling system, TC tracks are simulated by the track model with the genesis location and translation vectors, while the intensity evolution of TCs is calculated by the intensity model along the simulated tracks with the surrounding large-scale conditions (SST and vertical wind shear). The vertical wind shear is defined as the magnitude of the vector difference between monthly mean wind speeds at 850 hPa and 200 hPa. Further information about this technique can be found in Wang and Wu (2012).

3. Verification of the downscaling technique

The downscaling technique shows appreciable skill in reproducing the observed distributions of TC intensity and

tracks (Wang and Wu, 2012). To verify the downscaling technique, we first compare the observed and simulated TC track and intensity climatology. With the observed TC formation locations from JTWC, vertical wind shear, large-scale steering flows from NCEP–NCAR, and SST from NOAA, the track and intensity models are integrated to simulate the climatology of TC activity during the period 1975–2005. Note that the simulated TC track and intensity are independent of the observations from JTWC.

The observed and simulated TC tracks in the peak season are first compared (Fig. 1). In order to quantify the model bias in the track simulation, as defined in Wu and Wang (2004), the frequency of TC occurrence is calculated by counting the frequency of TCs entering each 2.5° latitude by 2.5° longitude grid box at 6-h intervals. This indicates the spatial pattern of TC tracks and estimates how frequently a region is influenced by TCs. It can be seen that the simulation reasonably reproduces the observed track climatology. The model slightly overestimates the frequency of occurrence over the ocean to the southeast of Japan and in the South China Sea (Fig. 2c), while the frequency of TCs affecting the East China Sea is underestimated. The discrepancies may result from the simplification of the TC steering flow by using monthly wind fields in the track model and/or the highly simplified track model.

The comparison between the observed and simulated spatial distribution of TC intensity is shown in Fig. 3. The TC intensity is defined as the mean surface wind speeds of those

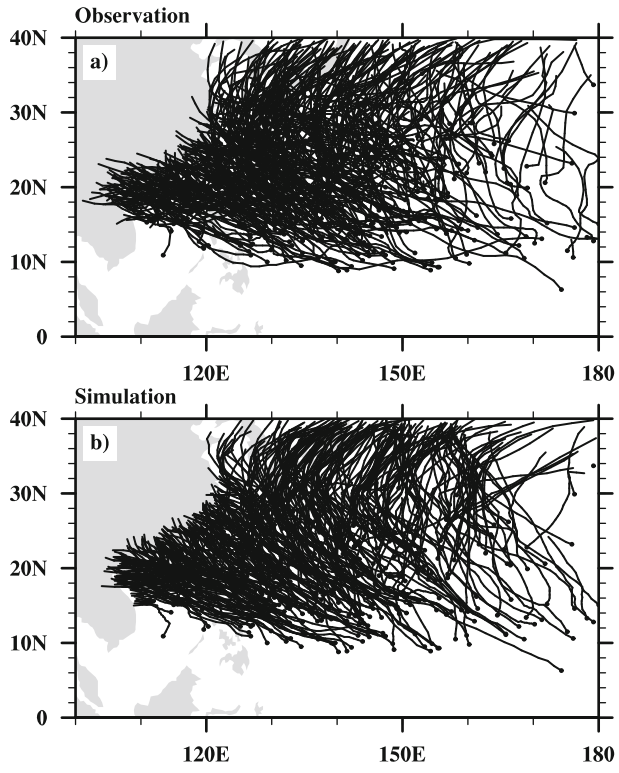

Fig. 1. TC tracks from July to September derived from (a) the JTWC best-track data and (b) the simulation during the period 1975–2005.

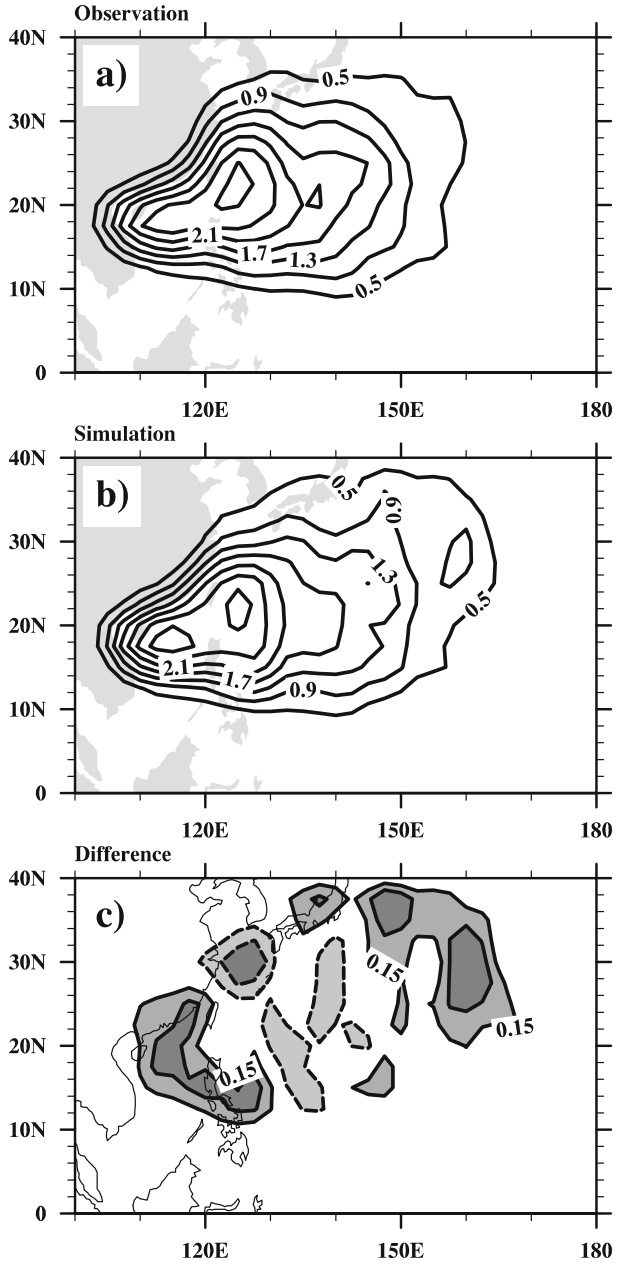

Fig. 2. Annual frequency of TC occurrence from July to September derived from (a) the JTWC best-track data, (b) the simulation, and (c) the difference between (b) and (a) during the period 1975–2005.

TCs that enter a grid box of 2.5° latitude by 2.5° longitude. As shown in Fig. 3, the overall spatial pattern of observed TC intensity, including the strong intensity band to the east of Taiwan, is reasonably well reproduced by the downscaling technique, although an overestimation of TC intensity exists in the midlatitude area (Fig. 3c). There are two possible sources of this discrepancy: one is owing to the absence of the extratropical transition and terrain effect in the downscaling system, and the other comes from the possible uncertainty in the TC intensity of the JTWC dataset (Kossin et al., 2007, 2013).

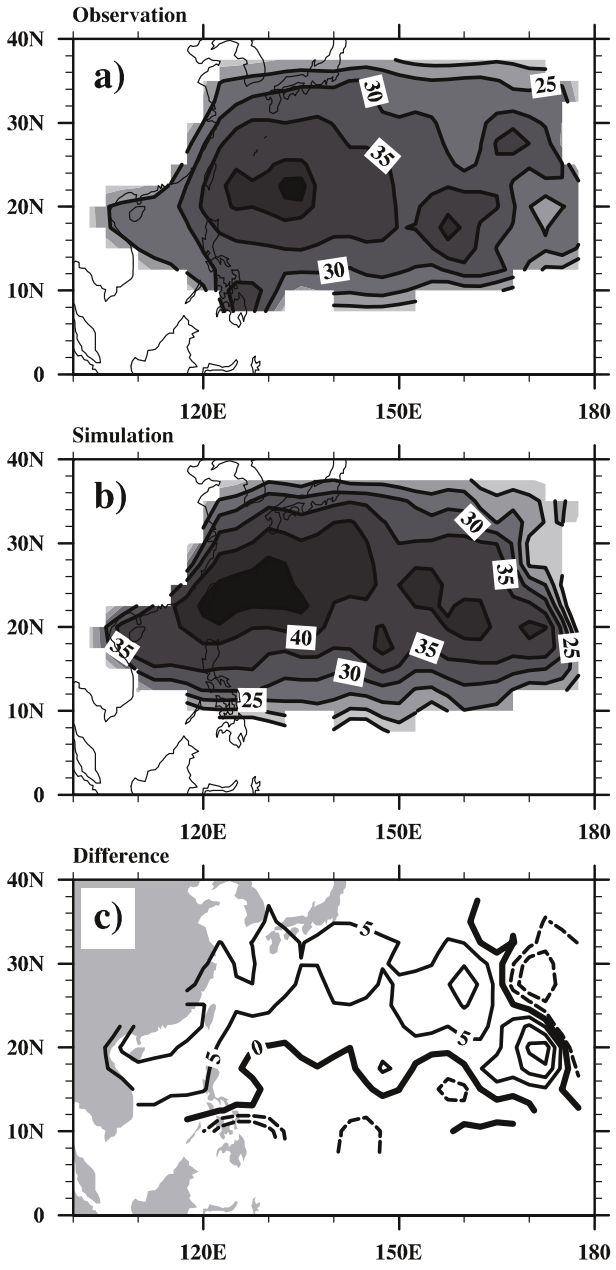

Fig. 3. Spatial distribution of TC intensity (units: m s^{-1}) derived from (a) the JTWC dataset, (b) the simulation, and (c) the difference between the simulation and the observation (contour interval: 5 m s^{-1}) in July–September during the period 1975–2005.

Following Wang and Wu (2012), the annual frequency of intense TCs (categories 4 and 5) and the lifetime maximum intensity are used to examine the possible influences of climate change on the basin-wide TC intensity. This is based on the indication by Wu and Zhao (2012) that these two metrics are more sensitive to the large-scale environment changes than the basin-wide average intensity (Wu et al., 2008). The annual lifetime maximum intensity is calculated by averaging the lifetime maximum intensity of individual TCs in each year (Wu, 2007). Figure 4 displays the differences between the observed and simulated time series of the annual basin-wide lifetime maximum intensity and the frequency of intense TCs. As can be seen, the evolution of the basin-wide TC intensity from 1975 to 2005 is also fairly well reproduced. The temporal correlation coefficients between the simulation and observation are 0.77 for the basin-wide lifetime maximum intensity, and 0.69 for the annual frequency of intense TCs, significant at the 95% level. In summary, the downscaling technique driven by the large-scale environment from NCEP–NCAR reanalysis data can reasonably reproduce TC track and intensity features over the WNP.

4. Selection of CMIP5 models

To evaluate the performance of CMIP5 climate models, we integrate the downscaling system driven by the large-scale environments (steering flows, vertical wind shear and SST) in their historical runs for the peak season during 1975–2005. The reliability of the CMIP5 climate models in simulating large-scale conditions for TC development is assessed by comparing the derived spatial distribution of the frequency of TC occurrence and TC intensity against the observation. Following Lee and Wang (2012), we calculate the normalized root-mean-square error (NRMSE) and pattern correlation coefficient (PCC) between the observation and simulation for each climate model over the WNP. The NRMSE is the root-mean-square error divided by the observed standard deviation. A higher PCC and smaller NRMSE imply that the simulation is closer to the observation.

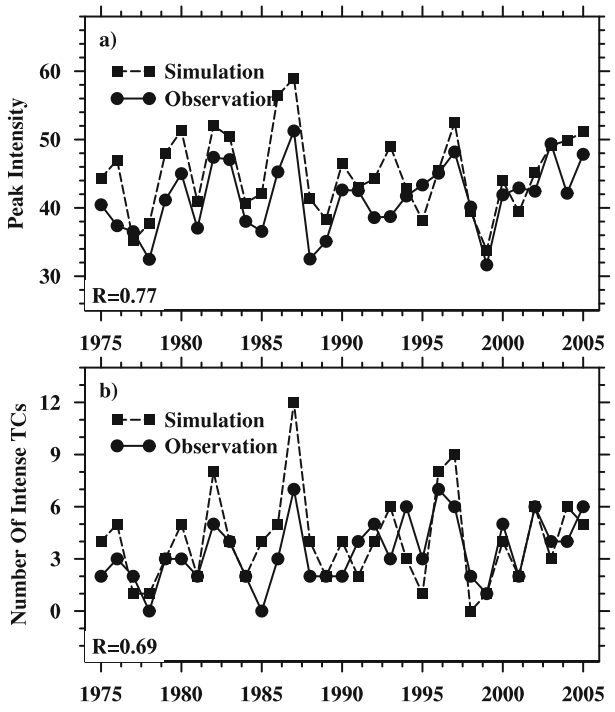

Fig. 4. Time series of (a) lifetime maximum intensity (units: m s^{-1}) and (b) the number of intense TCs from the JTWC dataset and the simulation during July–September during the period 1975–2005.

Figure 5 shows the calculated PCCs and NRMSEs of the individual CMIP5 models for the frequency of TC occurrence (Fig. 5a) and TC intensity (Fig. 5b). The average PCC (NRMSE) for frequency of occurrence is 0.75 (0.76), and the average PCC (NRMSE) for TC intensity is 0.64 (1.17). As shown in the figure, there is considerable inter-model spread in PCC and NRMSE. Considering both the skill of individual climate models and the sample size, the outputs from 11 CMIP5 models are selected (Table 1). Their RMSEs for frequency of TC occurrence (TC intensity) are less than 0.79 (1.21), while their PCCs for frequency of TC occurrence (TC intensity) are greater than 0.73 (0.66). Since the projected large-scale fields are not available for GFDL-CM2.1 and CMCC-CM, our projections are based on a final selection of nine CMIP5 models.

5. Projected changes in TC track and intensity

Compared to 1975–2005, the mean SST increase projected in the nine selected models is 0.6 K during 2010–29, 1.1 K during 2030–69 and 1.4 K during 2070–99 in the WNP basin. A control run is first performed with the large-scale conditions during 1975–2005 from the historical experiments of the selected climate models, followed by three projection runs with the mean large-scale conditions during 2010–39,

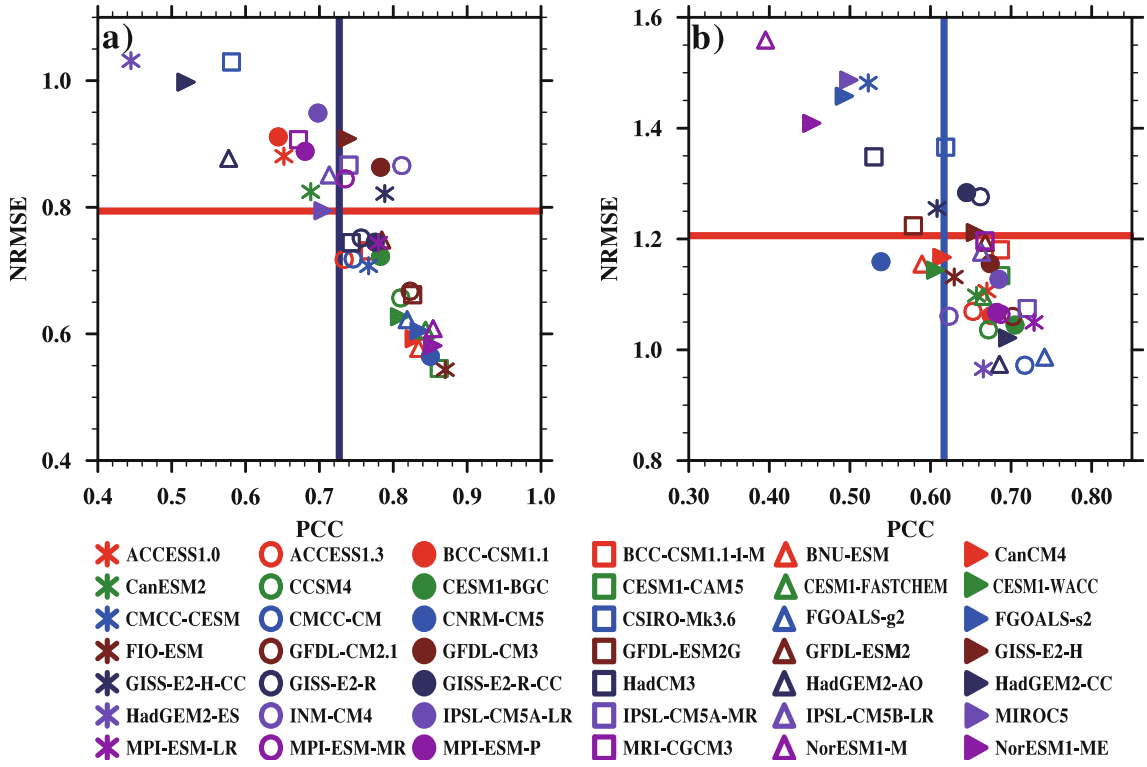

Fig. 5. Scatter plots of NRSME and PCC derived from individual GCMs: (a) frequency of TC occurrence; (b) spatial distribution of TC intensity. Red (blue) lines indicate the selection thresholds for NRSME (PCC).

Table 1. Description of the selected CMIP5 models.

Model	Number	Institution	Averaged atmospheric resolution (lon × lat, vertical levels)
ACCESS1.3	M1	Commonwealth Scientific and Industrial Research Organization and Bureau of Meteorology	1.875° × 1.25°, L17
BCC-CSM1.1-1-M	M2	Beijing Climate Center, China Meteorological Administration	1.125° × 1.25°, L17
CCSM4	M3	National Center for Atmospheric Research	1.25° × 0.94°, L17
CESM-BGC	M4	National Center for Atmospheric Research	1.25° × 0.94°, L17
CESM-CAM5	M5	National Center for Atmospheric Research	1.25° × 0.94°, L17
GFDL-ESM2M	M6	Geophysical Fluid Dynamics Laboratory	2.5° × 2.0°, L17
FIO-ESM	M7	The First Institute of Oceanography	2.8125° × 2.8125°, L17
FGOALS-g2	M8	Institute of Atmospheric Physics	2.8° × 3°, L17
MPI-ESM-LR	M9	Max Planck Institute for Meteorology	1.875° × 1.875°, L25
CMCC	M10	Centro Euro-Mediterraneo sui Cambiamenti Climatici	0.75° × 0.75°, L17
GFDL-CM2.1	M11	Geophysical Fluid Dynamics Laboratory	2.5° × 2.0°, L17

2040–69 and 2070–99. In each month, all of the formation locations that occurred in the corresponding month during 1975–2005 are used in the simulation.

5.1. *Track changes*

Figures 6a–c show the projected changes in the large-scale steering flow and the corresponding frequency of TC occurrence. Three climatological TC prevailing tracks are also plotted in this figure (Wu et al., 2005). A salient feature in the steering flow changes is an anomalous cyclonic circulation centered over the Taiwan Strait during the periods 2010–39 and 2040–69, and over Hainan Island during the period 2070–99. In response to the steering flow change, the common features for the three periods include decreasing TC activity in the South China Sea due to the enhanced westerly steering, and increasing TC activity in the East China Sea and northern part of Japan due to changes of the two prevailing tracks over the WNP. Since the annual TC counts are held fixed, the decreasing TC influence over the South China Sea suggests an increase in TCs that take a northwestward track. Note that the projected track changes are similar to the ensemble projection of five selected CMIP3 climate models under the A1B scenario (Wang et al., 2011). This is also consistent with previous observational analysis. Using the JTWC best-track dataset, Wu et al. (2005) found that the number of TCs affecting subtropical East Asia increased significantly during 1965–2003, while the South China Sea experienced decreasing typhoon influence. Recently, Tu et al. (2009) found that the influence of typhoons in the vicinity of Taiwan shows an abrupt increase after 2000. It is suggested that the observed track change will generally continue to the end of this century.

5.2. *Intensity changes*

Figures 7a and b show the percentage change in the lifetime maximum intensity and the frequency of intense TCs projected by each selected model for the three periods. The lifetime maximum intensity increases by 2.5%, 6.2% and

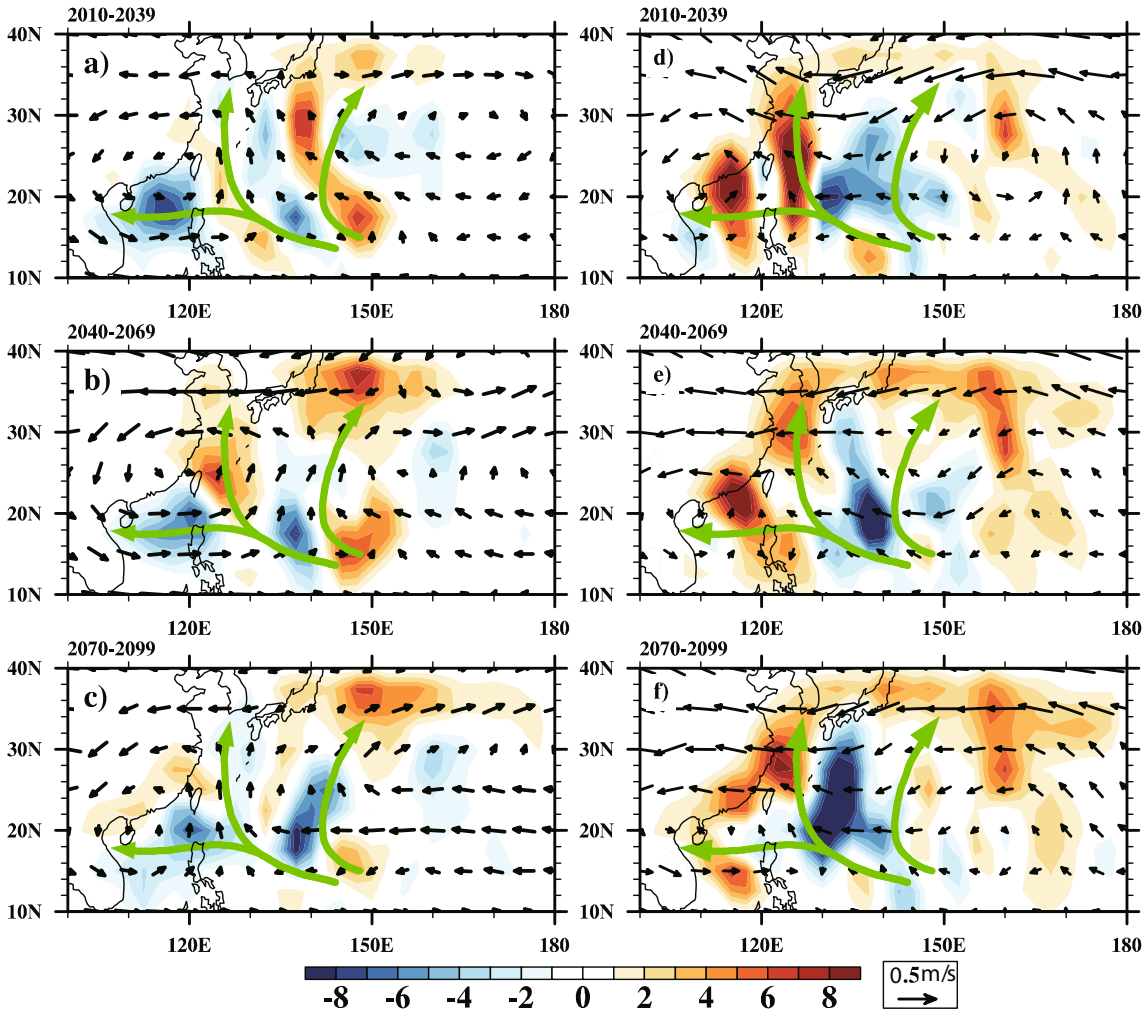

Fig. 6. Change in steering flow (black vectors) and the associated change in frequency of TC occurrence (shading) compared to the historical run for (a) 2010–39, (b) 2040–69, and (c) 2070–99 derived from the selected model ensemble. (d–f) As in (a–c), respectively, but derived from the selected model ensemble in Emanuel (2013). Green arrows show the climatological typhoon prevailing tracks from Wu et al. (2005).

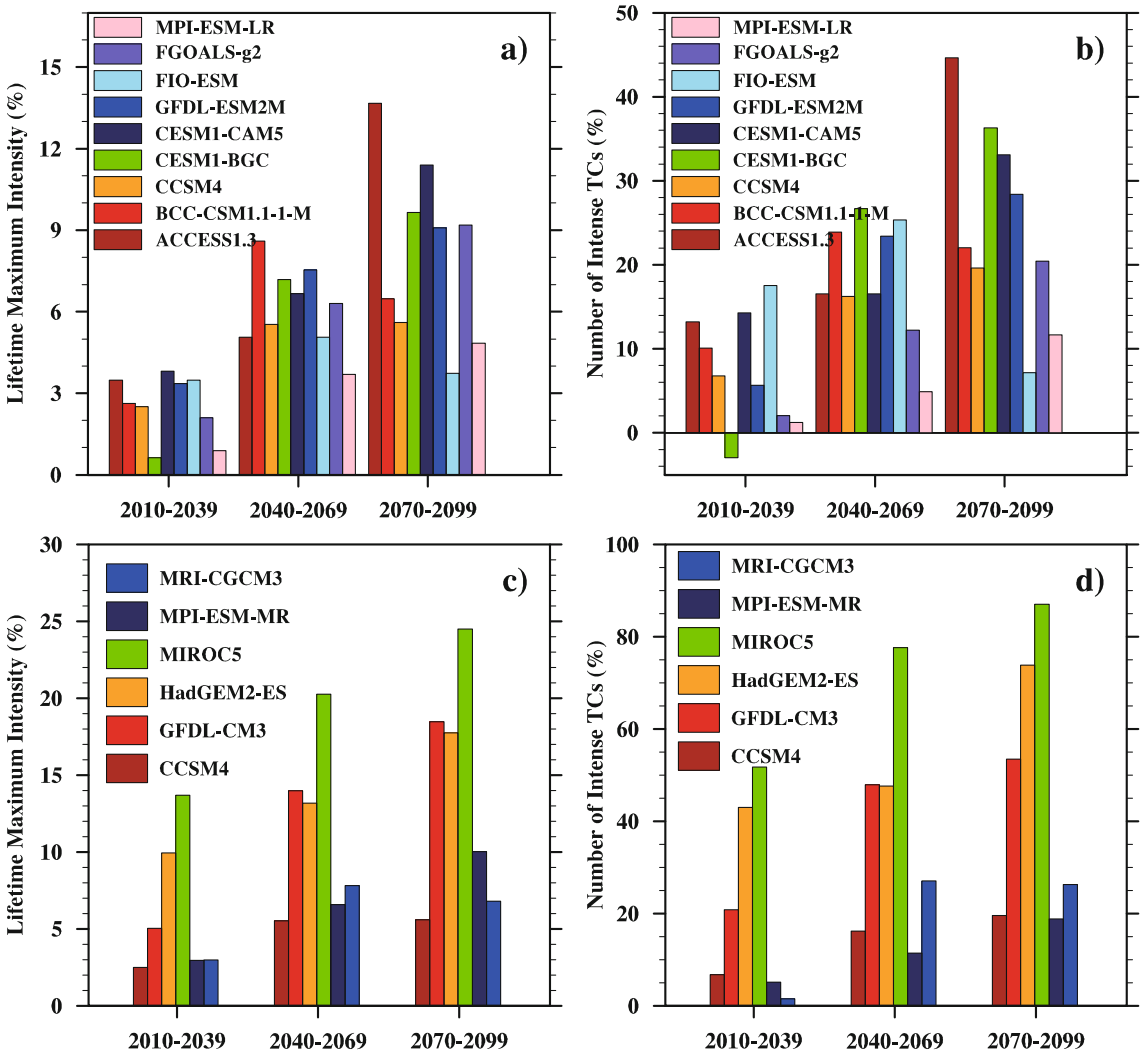

Fig. 7. Percentage changes in (a) the lifetime maximum intensity and (b) the number of intense TCs derived from each selected climate model. (c, d) As in (a, b), respectively, but derived from each selected model in Emanuel (2013).

8.2% as the mean SST increases by 0.6 K, 1.1 K and 1.4 K in the periods 2010–39, 2040–69 and 2070–99, respectively (Fig. 7a). In agreement with the increased lifetime maximum intensity, the number of intense TCs tends to increase under global warming (Fig. 7b). On average, the projected increases are 7.5%, 18.4% and 24.8% during the periods 2010–39, 2040–69 and 2070–99, respectively. The increases in the lifetime maximum intensity and the number of intense TCs are qualitatively in accordance with results derived from relatively high-resolution modeling and MPI theory (Emanuel, 1987; Knutson and Tuleya, 2004; Knutson et al., 2008; Emanuel et al., 2008, Knutson et al., 2010; Bender et al., 2010; Knutson et al., 2013; Emanuel, 2013).

5.3. *Contributions of track change*

As described in Wang and Wu (2012), the individual contributions of changes in TC prevailing track, SST and vertical shear to the intensity increase can be quantitatively examined by using a downscaling system. To examine the contribution of individual parameters, we can fix the other two parameters at their levels in the historical experiments, and only allow the target parameter to change in the 21st century. Although the combined effect of the individual parameters is not linear, it enables us to understand to what extent changes in TC prevailing tracks, SST and vertical wind shear can affect TC intensity changes (Fig. 8).

As shown in Fig. 8a, although its relative contributions are different in each model, the warming SST tends to intensify TCs in all of the selected GCMs during all three periods, which agrees with MPI theory (Emanuel, 1987; Holland, 1983). On average, increases of lifetime maximum intensity forced by SST are 3.5%, 6.3% and 8.5% during the periods 2010–39, 2040–69 and 2070–99, respectively. These changes are close to the changes with all parameters considered, suggesting that SST increase is the dominant factor causing increases in lifetime maximum intensity. On average, the changes in lifetime maximum intensity induced by the change of vertical shear (TC track) are −0.4% (−1.1%), −0.7% (−0.7%) and −0.5% (−0.9%) during the three periods, respectively.

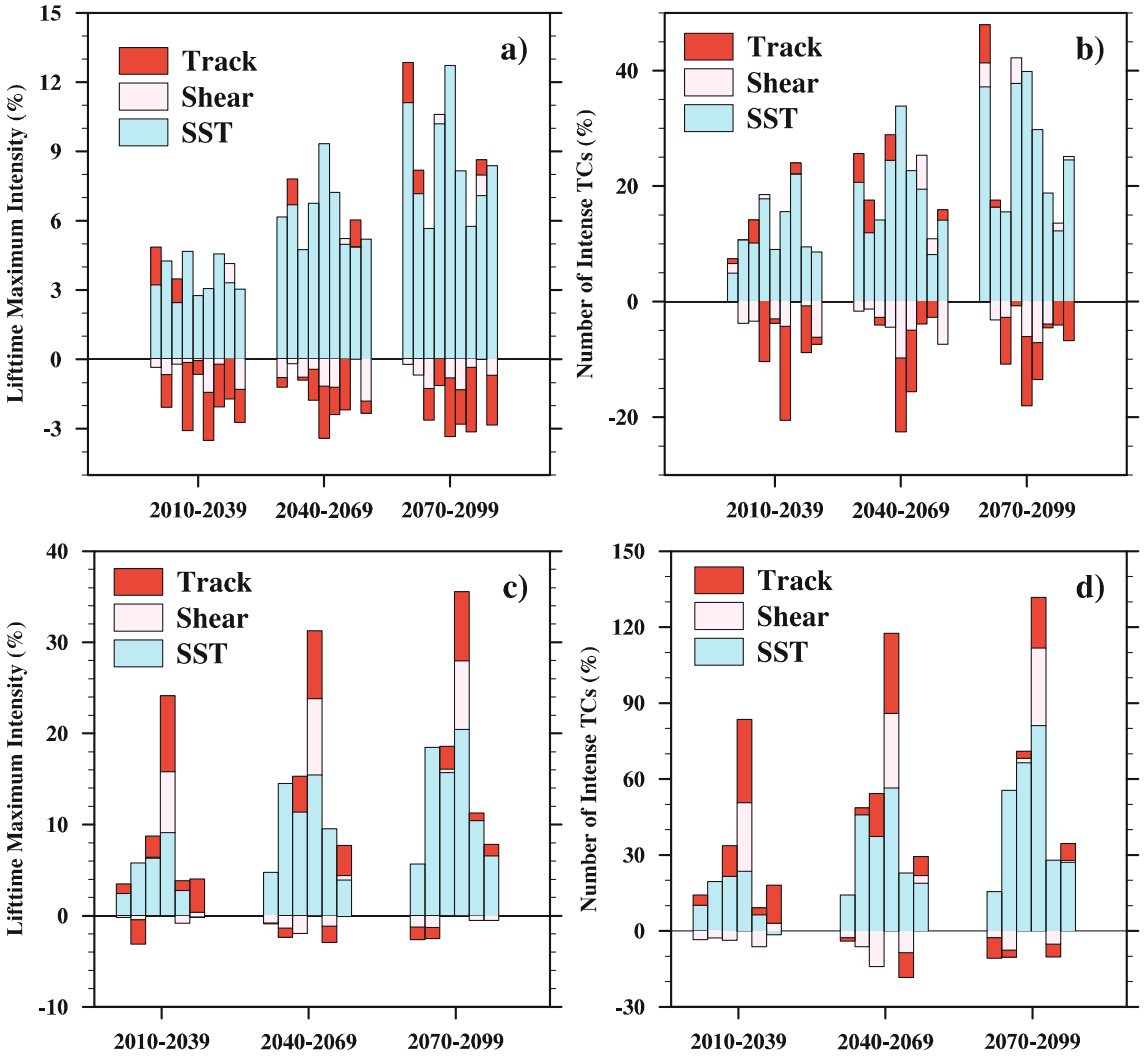

Fig. 8. Individual contributions from SST, vertical wind shear and prevailing tracks to the percentage change in (a) lifetime maximum intensity and (b) the number of intense TCs in each selected model. Each bar represents an individual model (M1–M9) of those presented in Table 1. (c, d) As in (a, b), respectively, but derived from each selected model in Emanuel (2013).

The joint influence of changes in prevailing track and vertical shear on intensity change is negative, accounting on average for 43%, 22% and 16.5% of the influence of SST warming in the three periods, respectively. Obviously, the percentage contribution of change in prevailing track and vertical shear to TC intensity decreases as SST gets warmer. The changes in vertical wind shear and prevailing track could significantly influence TC intensity in some models. For example, the composite effect of prevailing track and vertical shear change accounts for half of the increase in lifetime maximum intensity in the MPI-ESM-LR model during 2010–39, which is comparable to that of SST change.

The SST warming also acts as a predominant factor in the change of the number of intense TCs (Fig. 8b). The SST-forced increases in the number of intense TCs are 12%, 18.8% and 25.8% during the periods 2010–39, 2040–69 and 2070–99, respectively. In agreement with the lifetime maximum intensity, changes in prevailing track and vertical shear generally tend to reduce the number of intense TCs. The changes in the number of intense TCs induced by vertical wind shear (prevailing track) are −2.1% (−3.3%), −2.6% (−1.6%) and −1.4% (−3.4%) during the three periods. The combined negative contribution of change in prevailing track and vertical wind shear is on average about 45%, 23% and 17.4% of the contribution from SST warming in the three periods, respectively. The large contribution from changes in vertical wind shear and prevailing track suggests that those changes should be taken into account when assessing the impact of climate change on TC intensity. For instance, the majority of the positive contribution of SST warming to the change in frequency of intense TCs is offset by the combined negative contribution from the change in track and vertical shear in the CCSM4 model during 2079–99. In particular, the individual contribution from the prevailing track change in the GFDL-ESM2M model can reduce the number of intense TCs by 16.3%, which is slightly greater than the in-

crease (15.6%) due to SST warming during the first period. On average, the mean vertical wind shear over the area (5°–20°N, 115°–150°E) increases by 0.34, 0.37 and 0.03 m s^{-1} during 2010–39, 2040–69 and 2070–99, respectively, under the RCP4.5 scenario. Such increases in vertical wind shear are unfavorable to TC intensification, leading to the decreasing TC intensity. As shown in Fig. 6, TC influence in the South China Sea tends to decrease, and an increasing number of TCs take a northwestward track under a warmer climate. Considering the meridional SST gradient, the changes in prevailing tracks suggest that an increasing number of TCs would remain for less time over the tropical ocean with higher SST.

6. Sensitivity to model selection

In this study, we emphasize the evaluation and choice of the CMIP5 climate models appropriate for assessing the future change in TC activity. To demonstrate the importance, we examine the projected TC activity from the six climate models used in Emanuel (2013) (Table 2). Except for the CCSM4 model, the other five models in this table are not selected based on our criteria. It is shown that there are considerable differences in the projected change in TC track and intensity.

Figures 6d–f show the projected changes in the large-scale steering flow and frequency of TC occurrence during the periods 2010–39, 2040–69 and 2070–99. It is of interest to note that an anomalous cyclonic steering flow is also projected in these models, but the circulation center is slightly different from that in Figs. 6a–c. The center is around Hainan Island during the three periods. Instead of decreasing TC activity, the projection downscaled from the climate models in Emanuel (2013) shows increasing TC activity over the South China Sea, while the TC activity in the East China Sea is more enhanced than that from our selected climate models.

Figures 7c–d show the projected change in TC lifetime maximum intensity. The mean SST increases from the climate models selected in Emanuel (2013) are 0.7 K, 1.4 K and 1.8 K during 2010–39, 2040–69 and 2070–99, respectively, which are larger than the projections in our selection of models. As shown in Figs. 8c and d, the increases in lifetime maximum intensity (the number of intense TCs) are 6.2% (21.5%), 11.2% (38%) and 13.9% (46.5%) during the periods 2010–39, 2040–69 and 2070–99, respectively, which are nearly twice as much as in our selection of models, despite the fact that the SST increase is not doubled.

Similar sensitivity experiments to those carried out with the selected CMIP5 models are conducted, and the results are shown in Figs. 8c and d. On average, the changes in lifetime maximum intensity (the number of intense TCs) induced by SST are 4.4 % (13.2%), 9.9% (32.6%) and 12.9% (45.6%) during the periods 2010–39, 2040–69 and 2070–99. However, contrary to the projection based on our selected nine models, the changes in prevailing track and vertical wind shear in these six models generally tend to increase the TC intensity (Figs. 8c and d). The effect of changes in prevailing track can increase the lifetime maximum intensity (the number of intense TCs) by 2.3% (11.2%), 2% (8.0%) and 1.6% (2.3%), which are greater than the contribution from vertical shear [0.9% (2.3%), 0.6% (0.2%) and 0.7% (2.9%)] during the three periods, respectively. Note that the combined contribution from the change in prevailing track and vertical shear is comparable to the effect of SST warming during 2010–39. Moreover, the individual contributions of track changes even have a dominant influence on TC intensity change in some models. For example, the track change in the MIROC5 model increases the number of intense TCs by 32.9%, which is much greater than the 23.5% increase due to SST warming in the period 2010–39. In addition, the combined contribution of the change in track and vertical shear in the MIROC5 model is even larger than that of SST warming, which makes the MIROC5 model project the greatest increase in TC lifetime maximum intensity and intense TC numbers during the three periods among all the GCMs. In fact, this model is classified as one of the worst models for its poor performance in simulating both the spatial pattern of track density and intensity. The different results from these two sets of climate models suggest that a large spread exists in projections of future TC tracks and their contribution to intensity change in CMIP5 models.

7. Summary

The possible responses of TC tracks and their contribution to TC intensity change over the WNP in the future are quantitatively assessed using a downscaling technique based on the projected large-scale environments from CMIP5 cli-

Table 2. Description of the CMIP5 models selected in Emanuel (2013).

Model	Institution	Averaged atmospheric resolution (lon × lat, vertical levels)
CCSM4	National Center for Atmospheric Research	1.25° × 0.94°, L17
GFDL-CM3	Geophysical Fluid Dynamics Laboratory	2.5° × 2.0°, L23
HadGEM-ES	Met Office Hadley Center	1.875° × 1.25°, L17
MPI-ESM-MR	Max Planck Institute for Meteorology	1.875° × 1.875°, L25
MIROC5	Atmosphere and Ocean Research Institute, National Institute for Environmental Studies, and Japan Agency for Marine-Earth Science and Technology	1.4° × 1.4°, L17
MRI-CGCM3	Meteorological Research Institute	1.125° × 1.125°, L23

mate models under the RCP4.5 scenario. Specific attention is paid to evaluating and selecting the CMIP5 climate models based on the simulated large-scale environment for TC activity in their historical runs.

Due to changes in large-scale steering flows, the TC influence is projected to decrease in the South China Sea, with an increase in the number of TCs taking a northwestward track. With these changes in prevailing track, the projected TC lifetime maximum intensity (number of intense TCs) is increased by 2.5% (7.5%), 6.1% (18.4%) and 8.2% (24.8%) during the periods 2010–39, 2040–69 and 2070–2099, respectively. Meanwhile, the SST warming tends to increase the basin-wide TC intensity change as a dominant factor for most of the selected models; the simulated changes in prevailing tracks generally tend to counteract the effect of SST warming, which has a significant negative influence on TC intensity change in some models. The opposite effect of change in prevailing track and SST warming indicates that TC intensity cannot increase as estimated by MPI theory due to the contribution of TC track change.

To address the importance of model selection, we also examine the projected TC activity from the six CMIP5 climate models used in Emanuel (2013). Contrary to our results, increasing TC activity is projected over the South China Sea, with more TCs influencing the East China Sea. Despite the small difference in the projected SST increase, there are significant differences in the projected increases of the lifetime maximum intensity (number of intense TCs) between the six CMIP5 climate models used in Emanuel (2013) and our selected climate models due to the large positive contribution of the change in track and vertical shear. Since there is considerable inter-model variability in TC track and its contribution to intensity change, we suggest that model selection is important when assessing future TC activity.

Finally, it should be noted that this study assumes little change in TC formation location and frequency in future. However, several modeling studies have suggested that the global frequency of TCs may decrease under a warmer climate (e.g., Knutson et al., 2010), and thus caution should be applied when interpreting the results of our study.

Acknowledgements. The authors thank Prof. Kerry EMANUEL for allowing us to use his TC intensity model. This research was jointly supported by the National Basic Research Program of China (2013CB430103, 2015CB452803), the National Natural Science Foundation of China (NSFC; Grant No. 41275093) and the project of the specially-appointed professorship of Jiangsu Province. Chao WANG was also supported by the Research Innovation Program for College Graduates of Jiangsu Province (Grant No. CXZZ13_0496). This study is the Earth System Modeling Center Contribution Number 022.

REFERENCES

Bender, M. A., T. R. Knutson, R. E. Tuleya, J. J. Sirutis, G. A. Vecchi, S. T. Garner, and I. Held, 2010: Modeled impact of anthropogenic warming on the frequency of intense Atlantic hurricanes. *Science*, **327**(5964), 454–458, doi: 10.1126/science.1180568.

Emanuel, K. A., 1987: The dependence of hurricane intensity on climate. *Nature*, **326**, 483–485.

Emanuel, K., 2006: Climate and Tropical Cyclone Activity: A New Model Downscaling Approach. *J. Climate*, **19**, 4797–4802.

Emanuel, K. A., 2013: Downscaling CMIP5 climate models shows increased tropical cyclone activity over the 21st century. *Proceedings of the National Academy of Sciences of the United States of America*, **110**, 12219–12224.

Emanuel, K., R. Sundararajan, and J. Williams, 2008: Hurricanes and global warming: Results from downscaling IPCC AR4 simulations. *Bull. Amer. Meteor. Soc.*, **89**, 347–367.

Gray, W. M., 1968: Global view of the origin of tropical disturbances and storms. *Mon. Wea. Rev.*, **96**, 669–700.

Holland, G. J., 1983: Tropical cyclone motion: Environmental interaction plus a beta effect. *J. Atmos. Sci.*, **40**, 328–342.

IPCC, 2007. *Climate Change 2007: The Physical Science Basis. Contribution of Working Group I to the Fourth Assessment Report of the IPCC*, S. Solomon et al., Eds., Cambridge, UK. Cambridge University Press, 996 pp.

Kalnay, E., and Coauthors, 1996: The NCEP/NCAR 40-Year reanalysis project. *Bull. Amer. Meteor. Soc.*, **77**, 437–471.

Knutson, T. R., and R. E. Tuleya, 2004: Impact of CO_2-induced warming on simulated hurricane intensity and precipitation: Sensitivity to the choice of climate model and convective parameterization. *J. Climate*, **17**, 3477–3495.

Knutson, T. R., R. E. Tuleya, and Y. Kurihara, 1998: Simulated increase of hurricane intensities in a CO_2-warmed climate. *Science*, **279**, 1018–1020.

Knutson, T. R., J. J. Sirutis, S. T. Garner, I. M. Held, and R. E. Tuleya, 2007: Simulation of the recent multidecadal increase of Atlantic hurricane activity using an 18-km-Grid regional model. *Bull. Amer. Meteor. Soc.*, **88**, 1549–1565.

Knutson, T. R., J. J. Sirutis, S. T. Garner, G. A. Vecchi, and I. M. Held, 2008: Simulated reduction in Atlantic hurricane frequency under twenty-first century warming conditions. *Nature Geosci.*, **1**, 359–364.

Knutson, T. R., and Coauthors, 2010: Tropical cyclone and climate change. *Nature Geosci.*, **3**, 157–163.

Knutson, T. R., and Coauthors, 2013: Dynamical downscaling projections of Twenty-First-Century Atlantic hurricane activity: CMIP3 and CMIP5 Model-Based scenarios. *J. Climate*, **26**, 6591–6617.

Kossin, J. P., and S. J. Camargo, 2009: Hurricane track variability and secular potential intensity trends. *Climatic Change*, **97**, 329–337.

Kossin, J. P., K. R. Knapp, D. J. Vimont, R. J. Murnane, and B. A. Harper, 2007: A globally consistent reanalysis of hurricane variability and trends. *Geophys. Res. Lett.*, **34**, doi: 10.1029/2006GL028836.

Kossin, J. P., T. L. Olander, and K. R. Knapp, 2013: Trend analysis with a new global record of tropical cyclone intensity. *J. Climate*, **26**, 9960–9976.

Lee, J.-Y., and B. Wang, 2012: Future change of global monsoon in the CMIP5. *Climate Dyn.*, **42**, 101–119.

Li, T., M. Kwon, M. Zhao, J.-S. Kug, J.-J. Luo, and W. Yu, 2010: Global warming shifts Pacific tropical cyclone location. *Geophys. Res. Lett.*, **37**, L21804, doi: 10.1029/2010GL045124.

Murakami, H., B. Wang, and A. Kitoh, 2011: Future change of western North Pacific typhoons: Projections by a 20- km-

mesh global atmospheric model. *J. Climate*, **24**, 1154–1169.

Reichler, T., and J. Kim, 2008: How well do coupled models simulate today's climate? *Bull. Amer. Meteor. Soci.*, **89**, 303–311.

Smith, T. M., R. W. Reynolds, T. C. Peterson, and J. Lawrimore, 2008: Improvements to NOAA's historical merged land–ocean surface temperature analysis (1880–2006). *J. Climate*, **21**, 2283–2296.

Taylor, K. E., R. J. Stouffer, and G. A. Meehl, 2012: An overview of CMIP5 and the experiment design. *Bull Am Meteor Soc*, **93,** 485-498.

Tu, J.-Y., C. Chou, and P.-S. Chu, 2009: The Abrupt Shift of Typhoon Activity in the Vicinity of Taiwan and Its Association with Western North Pacific–East Asian Climate Change. *J. Climate*, **22**, 3617–3628.

Wing, A. A., A. H. Sobel, and S. J. Camargo, 2007: Relationship between the potential and actual intensities of tropical cyclones on interannual time scales. *Geophys. Res. Lett.*, **34**, doi: 10.1029/2006GL028581.

Wang, C., and L. Wu, 2012: Tropical cyclone intensity change in the Western North Pacific: Downscaling from IPCC AR4 experiments. *J. Meteor. Soc. Japan*, **90**, 223–233.

Wang, R., L. Wu, and C. Wang, 2011: Typhoon track changes associated with global warming. *J. Climate*, **24**, 3748–3752.

Wu, L. 2007: Impact of Saharan air layer on hurricane peak intensity. *Geophys. Res. Lett.*, **34**, doi: 10.1029/2007GL029564.

Wu, L., and B. Wang, 2004: Assessing impacts of global warming on tropical cyclone tracks. *J. Climate*, **17**, 1686–1698.

Wu, L., and B. Wang, 2008: What has changed the proportion of intense hurricanes in the last 30 years? *J. Climate*, **21**, 1432–1439.

Wu, L., and H. Zhao, 2012: Dynamically derived tropical cyclone intensity changes over the Western North Pacific. *J. Climate*, **25**, 89–98.

Wu, L., B. Wang, and S. Geng, 2005: Growing typhoon influence on East Asia. *Geophys. Res. Lett.*, **32**, L18703, doi: 10.1029/2005GL022937.

Wu, L., B. Wang, and S. A. Braun, 2008: Implications of tropical cyclone power dissipation index. *Int. J. Climatol.*, **28**, 727–731.

Zhang, Q., L. Wu, and Q. Liu 2009: Tropical cyclone damages in China 1983–2006. *Bull. Amer. Meteor. Soc.*, **90**, 489–495.